Molecular Crystals and Liquid Crystals

Publication details, including instructions for authors and subscription information:
http://www.tandfonline.com/loi/gmcl20

Polymer-dispersed Liquid Crystals: Effect of Partial Matrix Fluorination on Polymer Bead-based Morphology

M. D. Schulte [a b], S. J. Clarson [c], L. V. Natarajan [d], D. W. Tomlin [e] & T. J. Bunning [f]

[a] Materials and Manufacturing Directorate, Air Force Research Laboratory, MLPJ, WPAFB, OH

[b] Department of MS & E, University of Cincinnati, OH

[c] Department of MS & E, University of Cincinnati, Cincinnati, OH

[d] Science Applications International Corporation, Dayton, OH

[e] Technical Management Concepts, Inc., Beavercreek, OH

[f] Materials and Manufacturing Directorate, Air Force Research Laboratory, MLPJ, WPAFB

Version of record first published: 18 Oct 2010

To cite this article: M. D. Schulte, S. J. Clarson, L. V. Natarajan, D. W. Tomlin & T. J. Bunning (2002): Polymer-dispersed Liquid Crystals: Effect of Partial Matrix Fluorination on Polymer Bead-based Morphology, Molecular Crystals and Liquid Crystals, 373:1, 155-180

To link to this article: http://dx.doi.org/10.1080/10587250210531

Mol. Cryst. and Liq. Cryst., 2002, Vol. 373, pp. 155-180

Polymer-dispersed Liquid Crystals: Effect of Partial Matrix Fluorination on Polymer Bead-based Morphology

M. D. SCHULTE

Air Force Research Laboratory, Materials and Manufacturing Directorate/MLPJ, WPAFB, OH; Department of MS & E, University of Cincinnati, Cincinnati, OH

S. J. CLARSON

Department of MS & E, University of Cincinnati, Cincinnati, OH

L. V. NATARAJAN

Science Applications International Corporation, Dayton, OH

D. W. TOMLIN

Technical Management Concepts, Inc., Beavercreek, OH

T. J. BUNNING

Air Force Research Laboratory, Materials and Manufacturing Directorate/MLPJ, WPAFB

The morphology and electrooptical properties of polymer-dispersed liquid crystals (PDLCs) with partially fluorinated polymer matrices are investigated. Films were prepared via photo-induced free-radical polymerization of an initially isotropic solution comprised of pentafunctional (5 reactive groups) acrylate monomer and nematic liquid crystal molecules. Phase separation of discrete domains of LC is induced by the photopolymerization. The film morphologies consisted of aggregated polymeric particles dispersed throughout a continuous liquid crystal medium. Changes in morphology and electrooptical properties were observed as trifluoroethyl and hexafluoroisopropyl methacrylate were partially substituted for the multifunctional acrylate monomer. Methyl methacrylate was used in control films due to the chemical similarities to fluorinated monomers. The incorporation of fluorinated monomers resulted

Received 18 October 2000; accepted 14 May 2001.

The authors would like to acknowledge the United States Air Force for support through contract F33615-97-D-5405.

Address correspondence to Dr. T. J. Bunning, Senior Materials Research Engineer, AFRL/MLPJ, Bldg. 651, 3005 P Street, Suite 1, WPAFB, OH 45433-7702. Fax: (937) 255-1128; E-mail: Timothy.Bunning@wpafb.af.mil

in better definition of the polymer bead morphology and improvement in contrast ratio, while control films displayed less pronounced changes in optical properties. Real-time transmittance monitoring and polarized optical microscopy (POM) revealed that the monofunctional monomer addition resulted in a delay of the LC phase appearance with increasing comonomer concentration. However, a LC phase appeared earlier for fluorinated systems as compared to nonfluorinated control films of similar comonomer concentration. This was interpreted as an indication of lower LC solubility in the semifluorinated polymer matrix.

Keywords PDLC, fluorine, PIPS, morphology, gelation, electrooptical properties

INTRODUCTION

Polymer-dispersed liquid crystals (PDLCs) have received much attention over the past two decades due to their electrically switchable optical properties [1]. These composite materials consist of discrete liquid crystalline (LC) domains randomly dispersed throughout an amorphous polymer matrix in which nematic directors assume an overall random off-state orientation. In this state, the average refractive index of a spherical droplet is not equal to that of the surrounding polymer matrix leading to scattering of incident light. Upon application of an electric field, the LC directors become aligned parallel to the applied field and normal incident light passes through the film (for liquid crystals with positive dielectric anisotropy). The on-state transmittance is optimized when the polymer matrix and ordinary LC refractive indices are equal ($n_p = n_o$) [2].

Polymerization-induced phase separation (PIPS) is a convenient method to form LC domains within a polymer matrix. The polymerization may be driven by photochemical or thermal reactions. For either case, a reactive monomer is mixed with LC to form a homogeneous one-phase syrup. Polymerization leads to decreased solubility of the liquid crystal among polymer chains and the eventual formation of randomly dispersed droplets of liquid crystal in a polymer matrix. The resulting films can display a wide variety of morphological properties that are affected by formulation and polymerization conditions [3]. Photo-initiated PIPS is often favored over thermally initiated PIPS because manipulation of the final structure is relatively easy [4]. A wide range of morphologies is easily accessible via manipulation of the LC content and intensity of light.

PDLC films possess one of two extreme morphologies, either a ''Swiss-cheese'' or ''polymer-bead'' morphology. The former consists of LC droplets randomly dispersed in a continuous amorphous polymer matrix and is common in systems formed via step-growth polymerization [5] or low liquid crystal concentrations. These reactions are typified by the slow growth of

uniform polymer chains [6], and therefore LC molecules are eventually rendered insoluble and precipitate from the starting solution. Unlike step-growth polymerization, a chain-growth polymerization mechanism produces high molecular weight polymer in the early stages of the reaction [7]. When highly functional monomers (>3 reactive groups) are employed in combination with low LC concentrations ($<30\%$), the Swiss cheese morphology often prevails due to the highly crosslinked macroscopic network formed in the early stages of the reaction [8]. However, for formulations of intermediate or high LC concentrations, a polymer bead morphology is common [9]. In such cases, aggregated polymeric particles, often of varying degree of connectivity and shape, are dispersed randomly throughout a semicontinuous LC phase.

The mechanism of bead morphology formation has been described by Rajaram et al. [10] for high concentration systems (>97 wt% LC) using a tetrafunctional acrylate monomer and low molar mass liquid crystal. During the early stages of polymerization, the formation of nano- or micro-gel polymeric domains that are soluble in the syrup only at very low conversions occurs [10]. The miscibility gap is quickly breached and primary polymer particles precipitate and continue to grow amidst the syrup components, often in a reaction-limited growth process [11]. Eventually, the supply of monomers in the immediate vicinity of the polymer particles becomes depleted and the growth mechanism becomes diffusion-limited. Subsequent surface reaction of the primary particles results in aggregation, which leads to eventual macroscopic gelation, typically at low vinyl conversions ($<10\%$) [12]. The favorable electro-optical properties exhibited by these films are, in part, attributed to the dense polymeric domains and high LC volume fractions.

Floodlit films containing intermediate LC concentrations ($\approx 50\%$) are often desirable for display applications because the polymeric matrix imparts a high degree of mechanical integrity to the composite. However, films of this nature have two major disadvantages: 1) poor LC/polymer refractive index matching [13] and 2) small LC domains that result in high switching field requirements [14]. Several investigations have addressed similar problems in systems that exhibit the Swiss-cheese morphology [15]. The findings of these efforts have shown that the addition of fluorinated materials can improve contrast [16], enhance phase separation [17], and improve device response time [18]. These differences are attributed to decreased compatibility between hydrocarbon and fluorinated compounds and a reduction in the anchoring energy at the LC/polymer interface. However, no published works have examined the influence of fluorinated monomers on polymer bead PDLC morphology and electrooptical performance.

In a previous report by our group, fluorinated acrylate comonomers were demonstrated to have a significant impact on the morphological and electrooptical properties [19] of films formed with a pentafunctional acrylate monomer. The composition of these films was such that a polymer bead morphology was present. These films were observed to have improved contrast ratio over standard films, attributed to decreased chemical compatibility with partial matrix fluorination. The results are based on the bulk addition of a second monomer (fluorinated) into the polymer host. The objective of the research effort described in this article is to investigate the effect of a much slower reactive fluorinated comonomer, namely methacrylate-based monomers. It is hypothesized that the lower reactivity of a methacrylate vs. an acrylate monomer [20] may preferentially place the fluorine units at the polymer/LC interface. This approach of using two different monomers with unequal reactivity has been demonstrated in the past [21] to lead to localized differences in the polymer composition. A slower reacting monomer is preferentially segregated to the surface, thereby allowing control of the surface properties. Our approach is essentially the same, where a partial fluorination of the interface would be expected to substantially decrease the switching voltage and increase the relaxation switching time.

EXPERIMENTAL PROCEDURES

PDLC syrups consisted of an isotropic mixture of vinyl-terminated monomers, photoinitiator, coinitiator, and liquid crystals. The pentafunctional acrylate monomer was a mixture of 87 wt% dipentaerythritol pentaacrylate (DPHPA) and 13 wt% pentaerythritol tetraacrylate, both from Sartomer. This monomer was partially replaced with 1,1,1,3,3,3-hexafluoroisopropyl methacrylate (HFIPM) and 2,2,2-trifluoroethyl methacrylate (TFEM) to determine the effect of partial matrix fluorination on PDLC systems. For discussion purposes, the HFIPM is considered to have twice as much fluorine as the TFEM comonomer. Methyl methacrylate (MMA) and methyl acrylate (MA) were used as nonfluorinated control comonomers. The standard PDLC syrup consisted of 50 wt% inert liquid crystal E7 (EM Industries) and 50 wt% monomer. The latter consisted of 0.25 wt% photoinitiator Rose Bengal from Spectra Group, 2.0 wt% coinitiator *N*-phenylglycine (NPG), 16 wt% *N*-vinyl-2-pyrrolidinone (NVP) and the monomer mixture. 0–20 wt% HFIPM, TFEM, MMA, or MA were incrementally substituted for the multifunctional mixture to arrive at the various control and experimental formulations. NVP, MMA, MA, HFIPM,

TFEM, and NPG were purchased from Aldrich. All materials were used as received without further purification. A shaker mill was employed to mix all formulations so that homogeneity was ensured. After mixing, syrups were centrifuged for 1 min to remove dissolved gases.

Strict darkroom conditions were observed during PDLC cell preparations. ITO-coated glass slides were thoroughly cleaned with methanol prior to use. 15 μm glass spacer rods were utilized to achieve uniform film thickness, and these were deposited about the perimeter of an ITO-coated slide using methylene chloride (MC) as a carrying agent. After evaporation of the methylene chloride, approximately 25 μl of syrup was placed about the substrate center. A top slide was carefully placed over the first as to not entrap air bubbles between opposing glass plates. Excess syrup was then forced out through the sides of the cell. The assembled unit was placed in a custom-made aluminum holder that applied constant pressure to the perimeter of the cell during controlled irradiation.

Specimens were exposed for 8 min to a 315 mW/cm^2 light source originating from an unfiltered, 20 W incandescent halogen lamp. A randomly polarized HeNe laser beam ($\lambda = 632$ nm) offset 25° from the sample normal passed through the cell for real-time transmittance monitoring during writing and for 2 min thereafter. Samples were then removed from the holder and post-cured for 5 min at a distance of 6 in from an unfiltered, 50 W incandescent flood lamp.

Low-voltage, high-resolution scanning electron microscopy (SEM) was employed for morphology studies using a Hitachi S-900 scanning electron microscope operating in a secondary electron mode with a 1 keV accelerating voltage. Films were prepared for SEM analysis first by peeling them from the glass substrate with a razor blade and extracting the liquid crystal by immersing the free films in methanol for 12 h. The dried films were then mounted on metallic sample trays with silver paint followed by fracturing in liquid nitrogen to yield an interface that was representative of the bulk morphology. A 2–5 nm thick coating of tungsten was deposited on the surface of the specimen using a dual ion beam sputter coating system to minimize artifacts associated with sample charging.

A Nikon Optiphot-Pol polarizing microscope (POM) was employed to confirm the appearance of a LC phase and monitor events associated with real-time transmittance regimes. The microscope itself was not used to cure the films in situ. Threshold voltage, contrast ratio, and response times were assessed to determine film electrooptical performance. A 1 kHz AC square wave of known potential difference was placed across the thickness of the film. The threshold voltage, V_{90}, is defined as the voltage required for a

device to achieve 90% of its maximum transmittance (T_{max}). The rise time, τ_{on}, is defined as the time necessary for the minimum transmittance, T_{min}, to reach a value of $T_{min} + 0.9(T_{max} - T_{min})$. The relaxation time, τ_{off}, is defined as the time necessary for a device at T_{max} to return to a value of $T_{min} + 0.1(T_{max} - T_{min})$. These determinations were made by driving devices at their measured threshold voltages. The contrast ratio (CR) is a dimensionless parameter used to assess the on and off state optical performance of PDLC films and is defined as (T_{max}/T_{min}). Since these values are dependent on the optical performance in both the on and off states, each condition must be examined individually to provide insight into factors that affect film properties. The contrast ratio therefore serves as a means of making a general evaluation of optical performance.

RESULTS AND DISCUSSION

SEM was employed to study the morphology of the floodlit films. Figures 1a–c show that a porous polymeric phase (light regions) forms the structural

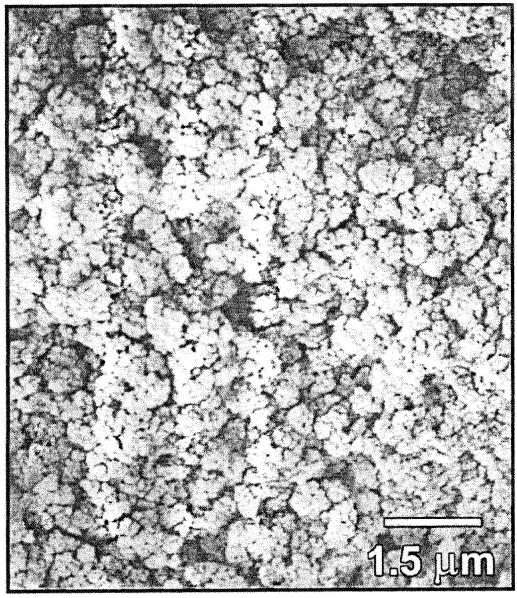

FIGURE 1 SEM photomicrographs of the standard formulation PDLC films at various magnifications.

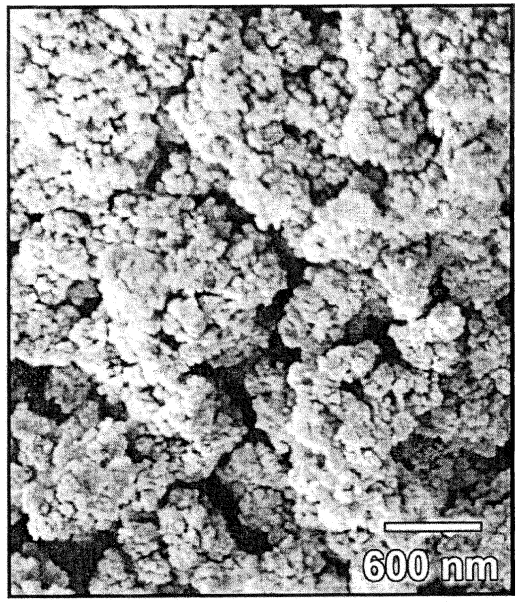

b.

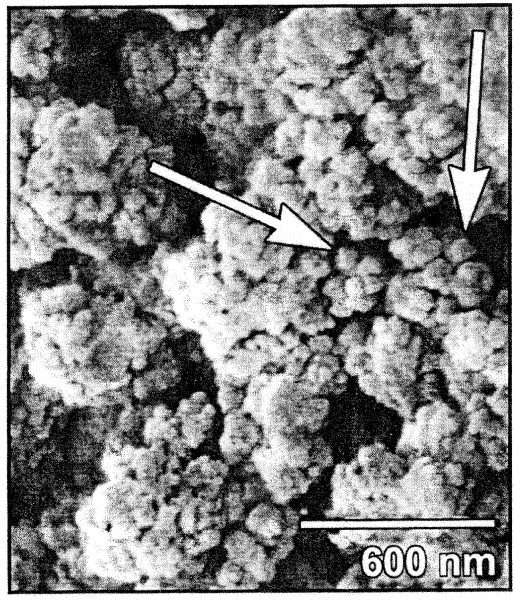

c.

FIGURE 1 (*continued*)

framework of standard films. The liquid crystal domains consist of irregularly shaped voids (dark regions). Closer examination reveals that the polymer film is comprised of interconnected clusters. Spherical polymeric particles measuring 50–70 nm in diameter form the basis of the aggregates and are analogous to the surface-reactive microgel particles described by Rajaram et al. [10, 22]. The free-radical polymerization mechanism coupled with the high functionality of the photo-reactive monomer cause small particles of very high molecular weight polymer to form early in the reaction. Because of the incompatibility of these beads with the syrup, precipitation occurs. Being surface-rich with functional groups, they continue to grow until a threshold to a diffusion-limited regime [9, 11] occurs. Neighboring beads then aggregate to form the final macroscopic network structure shown in Figure 1. For the base syrup, aggregation of the small polymer beads into 300–500 nm diameter clusters is evident. The size and shape of the LC domains is highly irregular. The largest LC voids are estimated to be 500 nm in diameter, although most voids are much smaller. Conventional PDLCs typically have much larger domains. The result of these small voids is demonstrated later by the relatively low contrast ratios and the high switching voltages observed for these films. The overall shape of the polymer clusters is highly irregular, and a considerable amount of surface roughness is present. These highly variable shapes suggest that the reaction of individual beads to a growing polymer cluster via surface reactive groups occurs preferentially over the continued reaction of monomer from the reacting polymer syrup. The latter would be expected to smooth the cluster interface, yielding more spherical aggregates. The transition from reaction-limited to diffusion-limited growth is characterized by slightly different morphologies [10]. For the former, dense compact structures exist, while for the latter a less dense, open-holed structure typically occurs. The morphology exhibited for the base syrup is clearly the latter and indicates that the morphology is dictated by the diffusion-limited probability of two beads reacting.

Figures 2 and 3 show the effect of adding approximately 11 mol% monofunctional monomer to the reactive mixture. Both figures correspond to the control (MMA-no fluorine), TFEM, and HFIPM at approximately similar compositions. These micrographs clearly indicate that as the concentration of fluorine is increased the volume fraction of LC increases, as evidenced by the larger fraction of dark void areas when compared to the base syrup. The spacing between individual polymer clusters increases and the largest LC domains are greater than 1 micron in length. Closer examination shows that the polymer clusters are comprised of primary

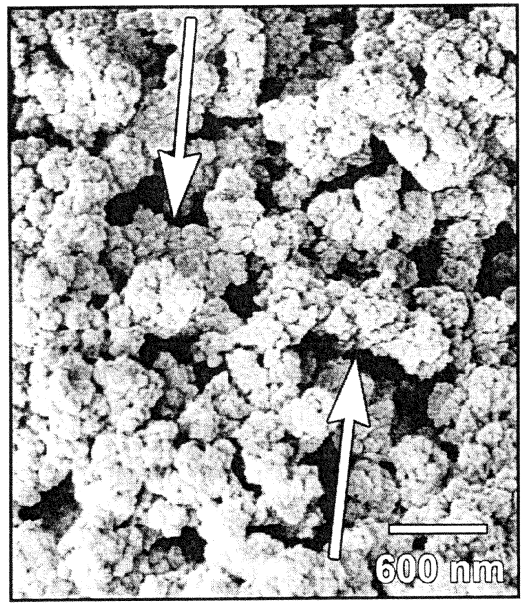

a.

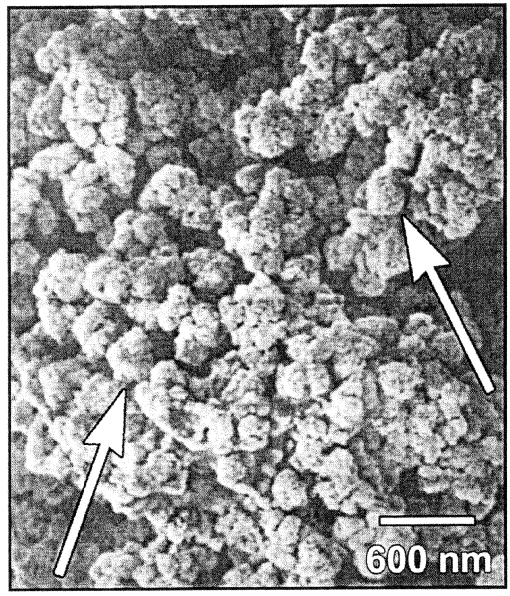

b.

FIGURE 2 SEM photomicrographs of (a) 11.6 mol% MMA, (b) 14.9 mol% TFEM, and (c) 11.1 mol% HFIPM PDLC films.

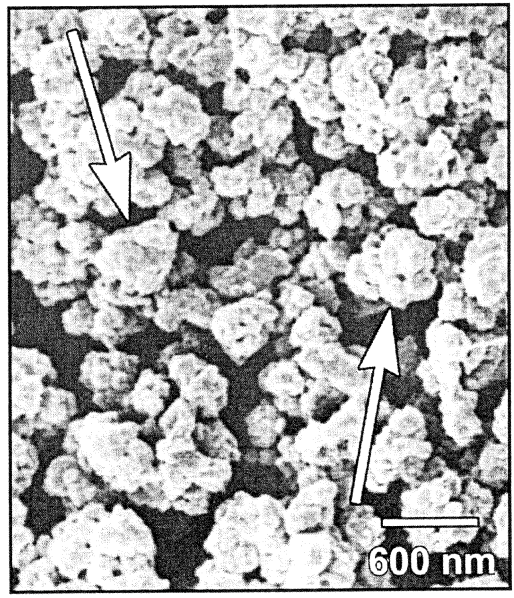

c.

FIGURE 2 (*continued*)

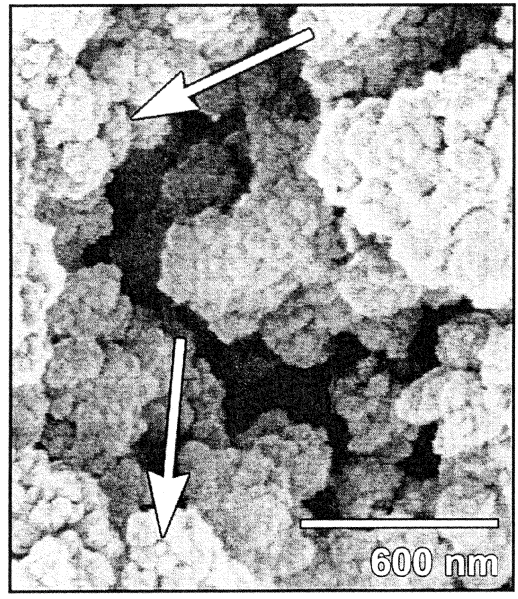

a.

FIGURE 3 SEM photomicrographs of (a) 11.6 mol% MMA, (b) 14.9 mol% TFEM, and (c) 11.1 HFIPM PDLC films.

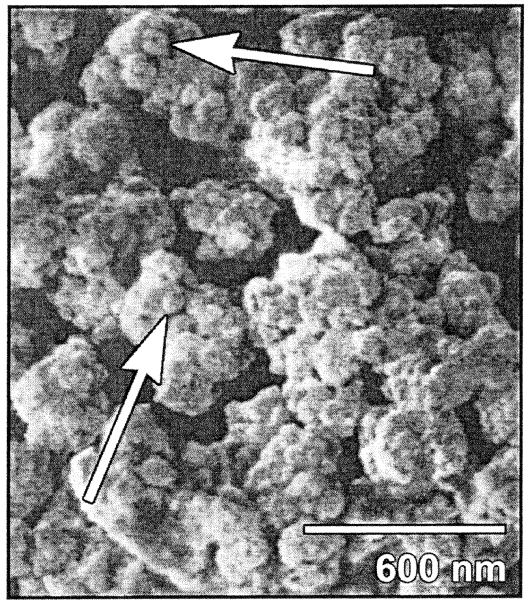

b.

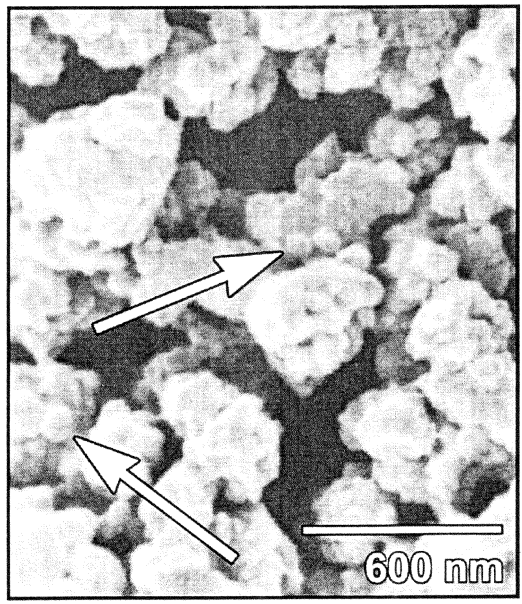

c.

FIGURE 3 (*continued*)

beads similar in size to those of standard formulation films (Figure 1). However, the compactness of the polymer clusters increases substantially with increasing fluorine content as evidenced by the much decreased surface roughness of the clusters. The amount of small holes within the clusters for the standard formulation films is greatly reduced upon addition of the alternative comonomers. Individual beads are still discernible within the clusters but the overall roughness of the clusters has decreased substantially.

In general, changes in morphological properties increased with increasing comonomer loading. This trend was observed for both nonfluorinated and fluorine-containing monomers. We attribute these observations to two separate phenomena. The increase in LC volume fraction is expected as the compatibility between the LC and polymer matrix would decrease upon fluorination. The presence of partial fluorination of the polymer matrix decreases the inherent solubility of the liquid crystal molecules in the polymer. The increase in compactness is attributed to differences in the reactivity between methacrylate and acrylate monomers. The addition of a monofunctional monomer acts as a reactive diluent (increasing the solubility of the LC), thereby causing phase separation to occur much later in time as compared to the base syrup. This is true regardless of the nature of the diluent and is attributed to decreased viscosity of the reactive syrup. The primary particles originate from the fast-reacting pentafunctional acrylate precursor in the nascent stages of polymerization. During this time, monofunctional comonomers act as a diluent imparting greater mobility to the beads and thus cause the transition from a reaction-limited to diffusion-limited condition to occur later in time. The structures that appear are therefore more dense and compact, as would be expected for a reaction-limited reaction condition [10].

The compact nature of the polymeric phase of fluorine-containing films is attributed to an appreciable degree of copolymerization between the acrylate matrix precursor and the methacrylate monomer [21]. As a result, liquid crystal components are less soluble in the partially fluorinated matrix and are more readily expelled during polymerization. This results in an increase in polymer bead density and a simultaneous increase in liquid crystal volume fraction.

The inherent reactivity of the comonomer is also important, as shown in Figure 4. Films formed using the MA comonomer are much closer in structure to the standard formulation films than films formed from the MMA comonomer. Although the addition of either monomer delays the onset to a diffusion-limited reactive condition, the decreased reactivity of the MMA comonomer delays the onset even further. Thus, at any given time

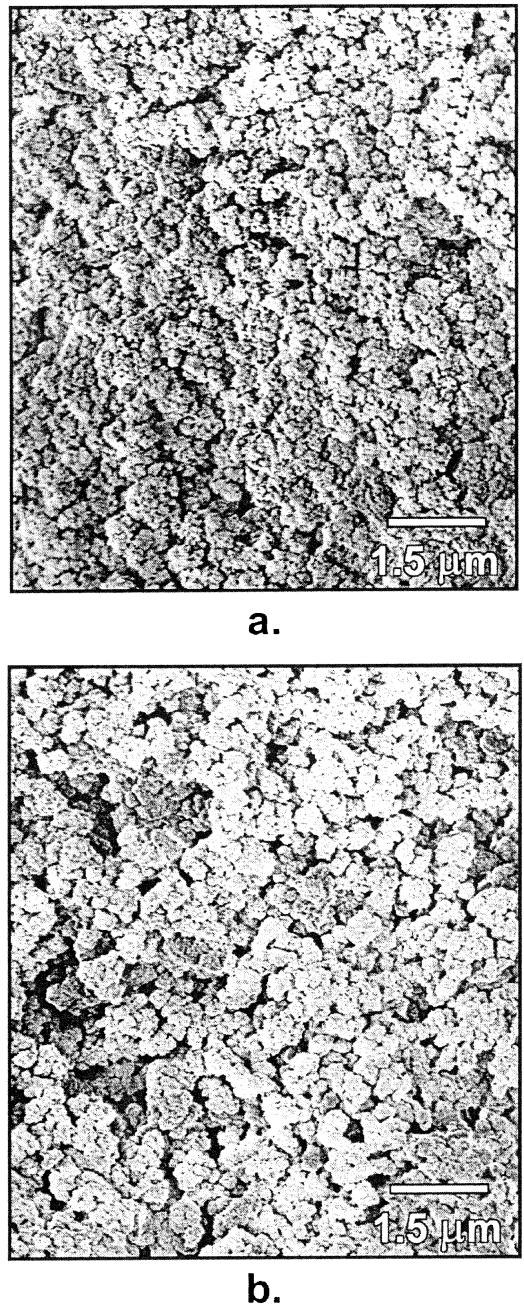

FIGURE 4 SEM photomicrographs of (a) 13 mol% MA, (b) 11.6 mol% MMA, (c) 13 mo1% MA, and (d) 11.6 mol% MMA PDLC films.

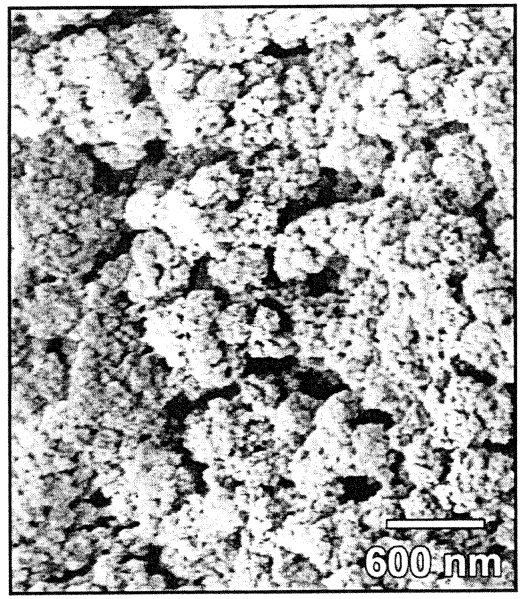

c.

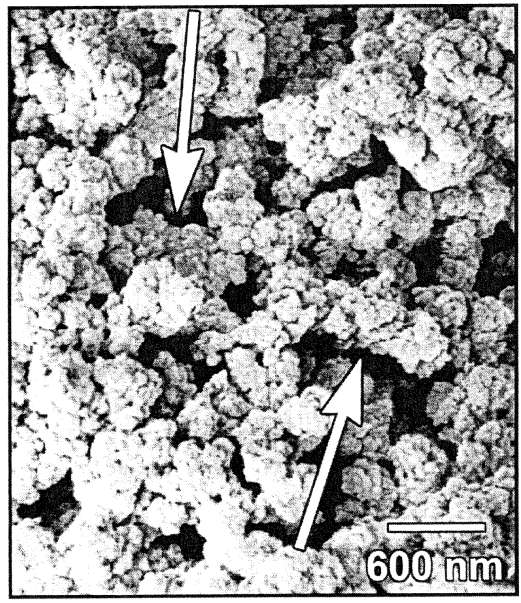

d.

FIGURE 4 (*continued*)

during the reaction, the concentration of MMA is greater than MA in the reacting syrup due to its decreased reactivity, resulting in lower syrup viscosity. Once the aggregate structure has been established, the continued reaction of MMA from a MMA-rich syrup would occur preferentially at the surface of these aggregates. This reaction at the surface smoothes the structure of the clusters as shown.

To explore the time dependence differences of the phase separation process, real-time scattering measurements were performed as the films were curing. The wavelength of the probing laser was outside the absorption characteristics of the visible dye system employed and thus did not contribute to the polymerization. Real-time transmittance monitoring was employed to qualitatively assess differences in component compatibility with comonomer concentration. Transmittance versus time plots of polymer-bead PDLC formation typically display three distinct regimes featured in the generalized scattering plot shown in Figure 5. All samples showed three separate regimes with large differences being observed between regimes one and two. Regime 1 denotes the beginning of specimen illumination and polymerization, leading to macroscopic gelation. Over the course of this regime, a slight haze gradually develops throughout the film. This haze is very weakly scattering with respect to the final film and, when viewed via POM, exhibits no birefringence. Because highly functional, free-radical systems precipitate high molecular weight polymer in the early stages of the reaction, it is presumed that concurrent changes in primary polymer particle and syrup refractive index gives rise to this scattering phenomenon. The films are mechanically stable at this point (i.e., they will not flow) indicating that macroscopic gelation has occurred. Eventually, a secondary haze appears in a wave that sweeps across the film denoted by the onset of regime 2. This wave was identified with optical microscopy as the appearance of a LC phase in which birefringent nuclei grow rapidly over the course of several seconds resulting in a sharp drop in transmittance. Thus, gelation occurs before the onset of LC birefringence. Regime 3 (after illumination ceases) is characteristic of dark polymerization.

The incremental addition of monofunctional monomers to the standard formulation results in a substantial delay in LC phase appearance (transition from regime 1 to regime 2) with increasing comonomer concentration, as shown in Figure 6. This is true for all monomers regardless of fluorine content, supporting the discussion earlier that these comonomers act as reactive diluents. The base syrup exhibits birefringence $\sim$1 min after illumination. As the concentration of comonomer is increased, the onset time steadily increases to $>$15 min. It is interesting to note that for any

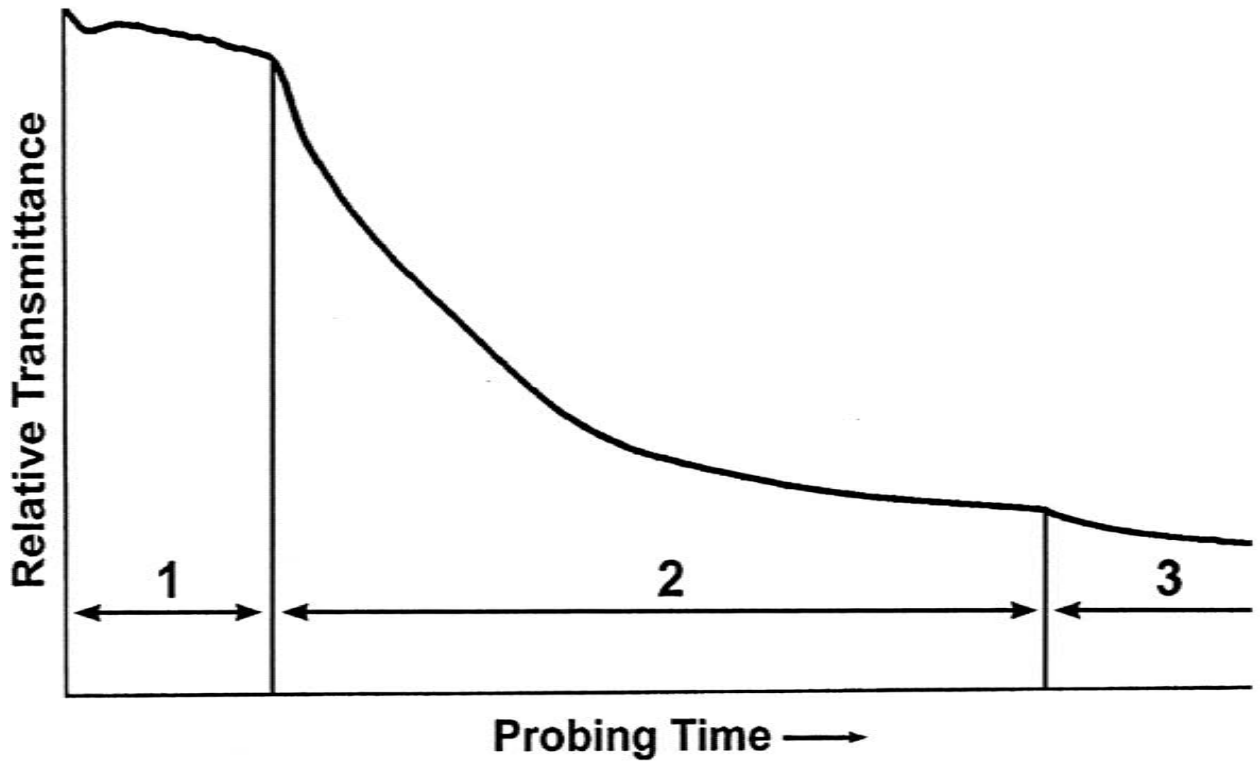

FIGURE 5 Generalized transmittance versus time curve for high-functionality, free-radically polymerized PDLC films.

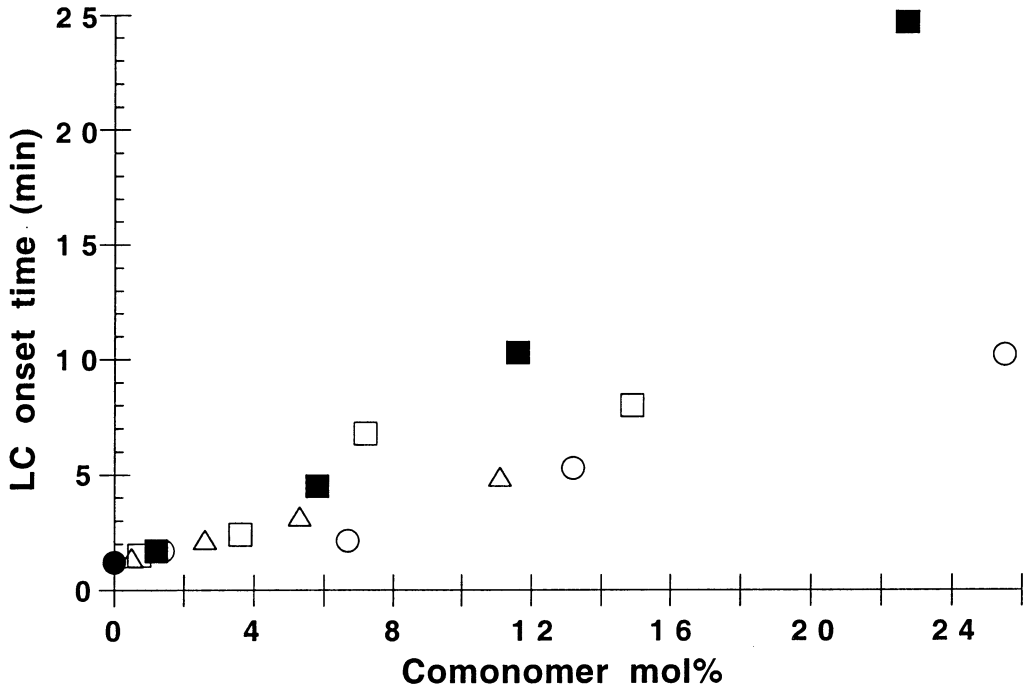

FIGURE 6 Liquid crystal phase appearance time versus comonomer mol% for standard formulation (●), MMA (■), MA (○), TFEM (□), and HFIPM (▲) PDLC films.

concentration of comonomer, the incorporation of fluorine causes the LC phase to occur earlier in time. Thus birefringence occurs first for HFIPM, TFEM, and finally MMA at a fixed concentration of comonomer. This is supportive of decreased solubility of LC within the partially fluorinated polymer matrix. Also shown in Figure 6 is the data for similar concentrations of the MA comonomer. The appearance of the LC phase much later in time for the MMA comonomer is attributed to a much lower reactivity. This is consistent with the morphology results presented earlier. At any given time during the reaction, the reactive mixture has more methacrylate comonomer than in the corresponding acrylate case. Given that the LC will be much more soluble in a low molar mass diluent than the polymer beads, the LC preferentially resides in the reactive syrup.

As shown, the addition of MMA-based comonomers has large effects on the resulting morphology when compared to the standard formulation films. To explore whether these differences had an appreciable effect on the electrooptical properties, contrast ratio, switching voltage, and relaxation time measurements were performed as a function of composition. The standard formulation films had an average contrast ratio of 7.6, as shown in Figure 7. The measurements performed here were conducted after 10 days of aging to ensure all post-polymerization changes had occurred. The absolute numbers are not meant to be compared with values needed for commercial films but instead are meant for comparison purposes. All results were taken as the average value of three films and plotted as a function of comonomer mol%. The addition of MMA at all concentrations had no appreciable effect on the contrast ratio. The addition of TFEM results in a more than twofold increase in contrast ratio, suggesting that the incorporation of fluorine is important. A dramatic increase in contrast ratio is observed with the addition of HFIPM for a maximum value of 70.3. For both fluorinated comonomers, the contrast ratio increased with comonomer concentration. Although the morphology results showed differences between monomers, the large difference in contrast ratio values is intriguing. To investigate the origins of the large differences, both $T_{\min}$ and $T_{\max}$ are examined individually for each comonomer series.

The base syrup films displayed an average on-state transmittance of 88%. A general increase in $T_{\max}$ with increasing comonomer concentration is observed for both fluorinated and nonfluorinated monomers, as shown in Figure 8a. Little difference between fluorinated and nonfluorinated monomers exist. $T_{\max}$ is related to how well the refractive index of the polymer matrix and phase separated LC domains match. The average off state ($T_{\min}$) transmittance of standard formulation films was determined to be 12%.

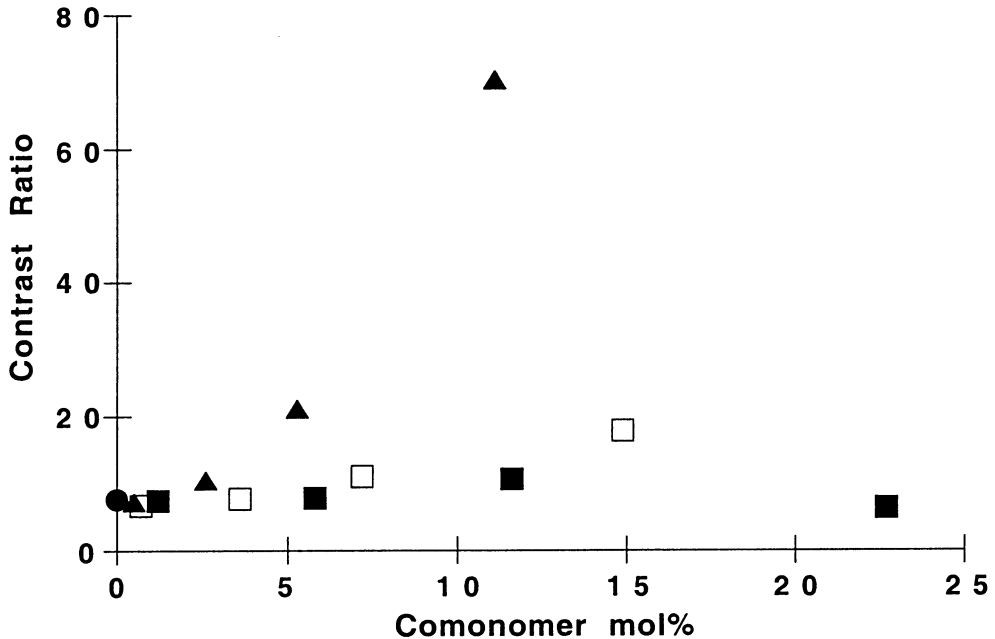

FIGURE 7 Contrast ratio versus comonomer mol% for standard formulation (●), MMA (■),TFEM (□), and HFIPM (▲) PDLC films.

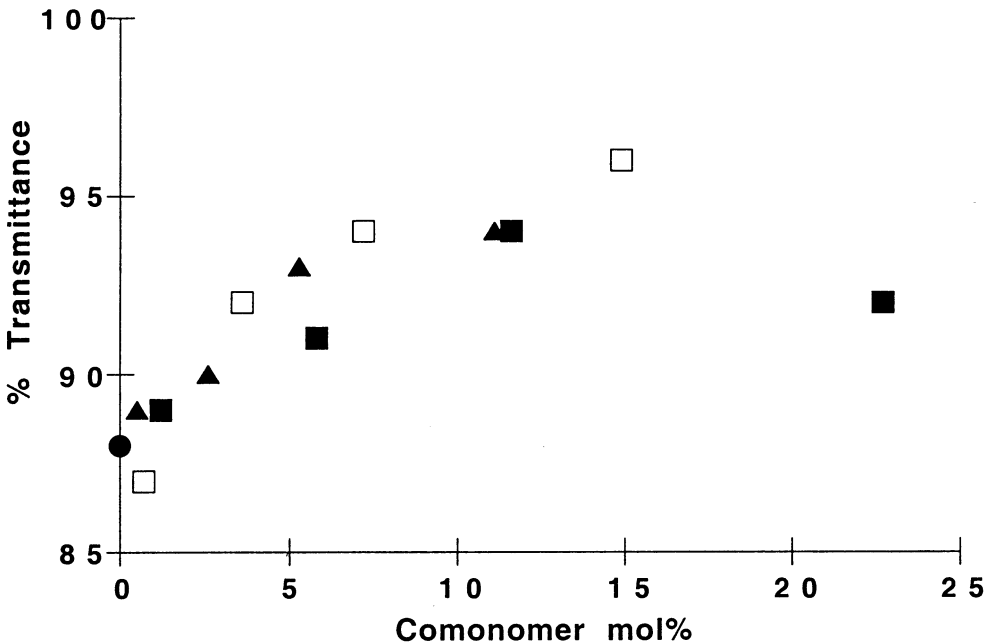

FIGURE 8 (a) On state transmittance versus comonomer mol% for standard formulation (●), MMA (■), TFEM (□), and HFIPM (▲) PDLC films. (b) Off state transmittance versus comonomer mol% for standard formulation (●), MMA (■), TFEM (□), and HFIPM (▲) PDLC films.

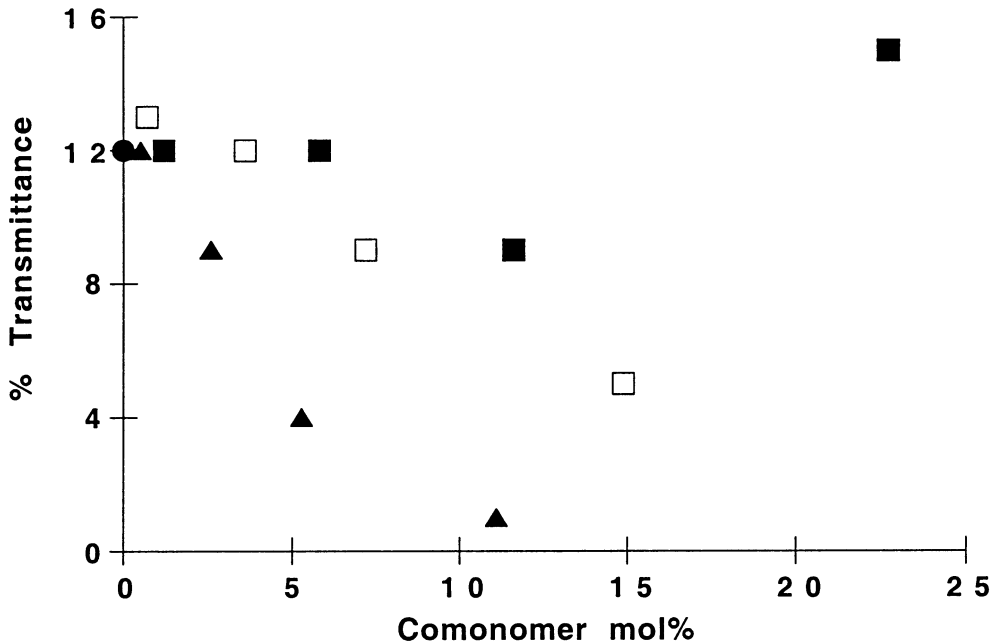

FIGURE 8 (*continued*)

Large differences were observed with comonomer as the off- state transmittance generally decreased with increasing concentration, as shown in Figure 8b. In addition, large differences were observed as the most fluorinated comonomer (HFIPM) had a much greater effect than MMA. These minimum transmittance values are related to the scattering power of these films, which is related to the average difference in refractive index and domain size. Thus, the reason for significant contrast ratio improvements with the addition of fluorinated comonomers is due to decreased off state transmittance with matrix fluorination.

The addition of monofunctional monomers to the syrup results in an overall decrease in matrix refractive index with increasing comonomer concentration [19]. This results in improved matching between the ordinary liquid crystal and polymer matrix refractive indices (n_o and n_p, respectively), thereby improving the on state transmittance. Polymer matrix and liquid crystal impurities as well as curvature about the liquid crystal/polymer interface result in a maximum transmittance that is less than optimal. Conversely, the off state scattering properties of fluorinated films increased, as indicated by the decrease in transmittance. Relatively little change is observed for the nonfluorinated comonomer. This is due to an increase in refractive index between the polymer matrix and unaligned liquid crystal domains (n_p and n_{LC}, respectively). In addition, the increases in polymer bead size and liquid crystal volume fraction further improve the scattering characteristics of fluorinated films. Nonfluorinated control films, on the other hand, revealed a decrease in scattering properties with increasing comonomer concentration. This is attributed to a high concentration of nonfluorinated monomer dissolved in the liquid crystal domains, thereby lowering the effective refractive index, n_{LC}, and better matching it to that of the polymer matrix, n_p.

Switching experiments were conducted to investigate possible changes in the threshold voltage with fluorination. Standard formulation PDLC films possessed an average threshold voltage of 10.8 V/μm, as shown in Figure 9. The high driving voltage is largely attributed to the submicron domain sizes, as indicated by the SEM micrographs. Since the voltage needed to reorient liquid crystal molecules scales inversely with domain size, the small, surface-rich voids present for these beadike morphologies would be expected to yield high switching voltages. The addition of MMA results in a systematic decrease in V_{90} down to 3.5 V/μm. This represents a maximum driving voltage reduction of threefold. Reduction in the driving voltage is also observed for the fluorinated comonomers, although generally smaller than the MMA cases. In general, the decrease in switching voltage can be related

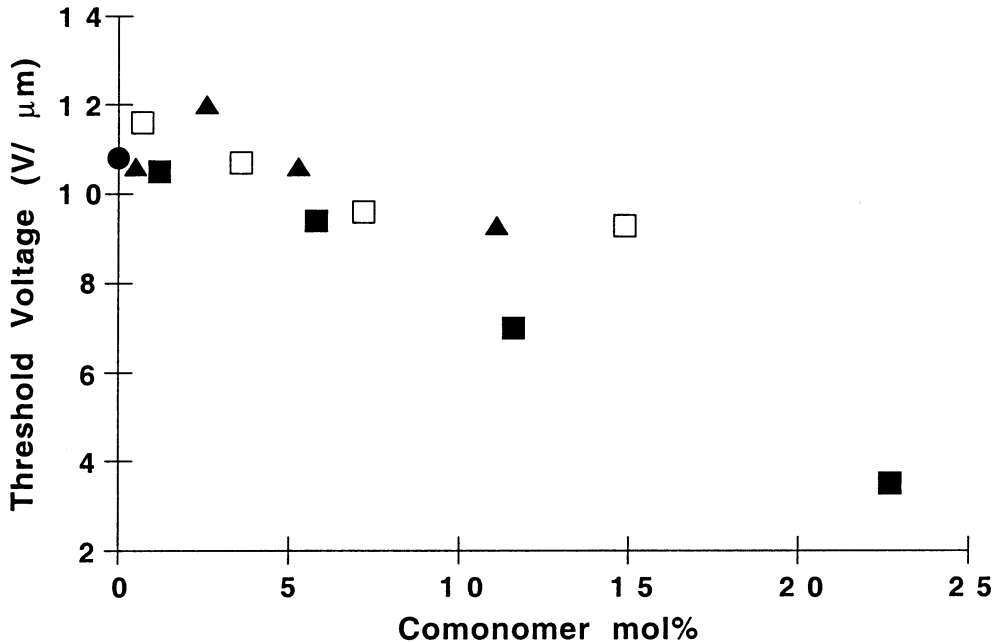

FIGURE 9 Threshold voltage (V_{90}) versus comonomer mol% for standard formulation (●), MMA (■), TFEM (□), and HFIPM (▲) PDLC films.

to size and shape of the LC domains. Since increasing the LC volume fraction leads to larger domains, the general reduction with concentration for all comonomers is expected. The fact that no systematic difference occurs upon fluorination suggests that the polymer interfaces are NOT significantly fluorine rich.

To further confirm that no preferential fluorination of the interface has occurred, relaxation time measurements were obtained. The relaxation time or τ_{off}, is governed by a balance between the surface anchoring energy, elastic free energy, and LC viscous torque. In general, a reduction of the anchoring energy expected with surface fluorination would increase the relaxation time. The reduction in anchoring energy would reduce the strength of the elastic, restoring force, and driving the directors back to their initial orientations in the field off state. Standard formulation films possess an average relaxation time of 156 μs. A small general increase in τ_{off} is observed with increasing comonomer concentration as shown in Figure 10 with each series displaying maximum relaxation times between 205 and 250 μs. This is consistent with the slightly increased LC volume fraction (void size) as the comonomer concentration is increased. The fact that no difference exists between MMA and the two fluorinated monomers suggests little difference in the anchoring strength. Thus, both the switching voltage and relaxation measurements do not indicate that the interfaces are fluorine rich.

CONCLUSIONS

The addition of fluorinated methacrylate monomers was demonstrated to have significant effects on morphological and optical properties of PDLC composites formed with photopolymerization. The morphology of PDLC films with methacrylate monomers displayed enhanced phase separation manifested in an increased LC volume fraction. However, a high degree of comonomer fluorine substitution produces more dramatic morphological effects for low concentration due to decreased component compatibility as verified by real-time transmittance studies. Due to enhanced phase separation and increased incompatibility with partial matrix fluorination, improvements in contrast ratio were also realized. These were attributed to favorable changes in morphological properties with partial fluorination. No indication of preferential fluorination of the polymer/LC interfaces due to the lower reactivity of methacrylate monomers was observed.

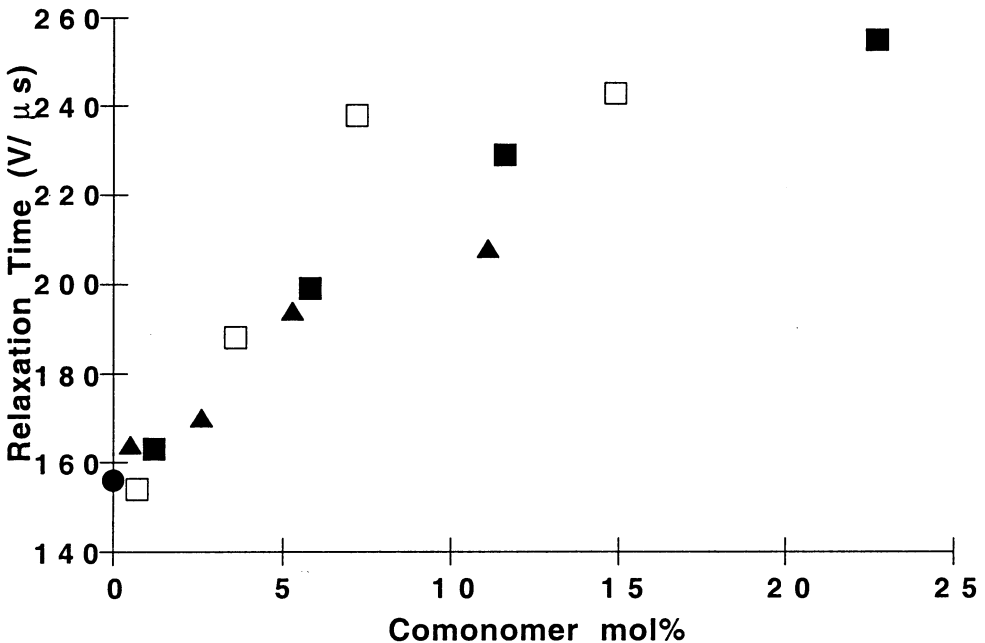

FIGURE 10 Relaxation time versus comonomer mol% for standard formulation (●), MMA (■), TFEM (□), and HFIPM (▲) PDLC films.

ACKNOWLEDGEMENTS

This work was performed at the Air Force Research Laboratory, Wright-Patterson Air Force Base, OH. The authors wish to thank Mr. Greg Hostetter from the University of Cincinnati for conducting polarized optical microscopy studies.

REFERENCES

1. P. S. Drzaic, *Liquid Crystal Dispersions* (World Scientific, River Edge, New Jersey, 1995).
2. S. Zumer and J. W. Doane, *Phys. Rev. A*, 34, 3373–3380 (l986).
3. D. K. Yang and J. W. Doane, *SID Tech. Paper Digest*, 23, 759–786 (1992).
4. C. V. Rajaram, S. D. Hudson, and L. C. Chien, *Photonic and Optoelectronic Polymers*, 672, 320–337 (American Chemical Society, Washington, DC, 1997).
5. A. M. Lackner, J. D. Margerum, L. J. Miller, F. G. Yamagishi, E. Ramos, K. C. Lim, K. W. H. Smith and C. I. Van Ast, *SID Proc.*, 32, 173–177 (1991).
6. P. C. Painter and M. M. Coleman, Polymer Synthesis, in *Fundamentals of Polymer Science*, (Technomic Publishing Co. Inc., Lancaster, Pennsylvania 1994).
7. H. R. Allcock and F. W. Lampe, *Condensation and Other Step-Type Polymerizations, chapter 2*, (Prentice Hall, New Jersey, 1990).
8. T. J. Bunning, L. V. Natarajan, V. P. Tondiglia, R. L. Sutherland, R. Haaga, and W. W. Adams, *SPIE Proc.*, 2651, 44–52 (1996).
9. C. V. Rajaram, S. D. Hudson, and L. C. Chien, *Chem. Mater.*, 8, 2451–2460 (1996).
10. C. V. Rajaram, S. D. Hudson, and L. C. Chien, *Chem. Mater.*, 7, 2300–2307 (1995).
11. C. V. Rajaram, S. D. Hudson, and L. C. Chien, *Morphology of Composites of Low-Molar-Mass Liquid Crystals and Polymer Networks* (American Chemical Society, Washington, DC, 1997).
12. R. T. Pogue, L. V. Natarajan, V. P. Tondiglia, S. A. Siwecki, R. L. Sutherland, and T. J. Bunning, *SPIE Proc.*, 3475, 2–11 (1998).
13. M. D. Schulte, S. J. Clarson, L. V. Natarajan, V. P. Tondiglia, and T. J. Bunning, *Mat. Res. Soc. Symp. Proc.*, 559, 135–140 (1999).
14. B. G. Wu, J. H. Erdmann, and J. W. Doane, *Liquid Crystals*, 5, 1453–1465 (1989).
15. L. V. Natarajan, R. L. Sutherland, V. P. Tondiglia, T. J. Bunning, and W. W. Adams, *J. of Nonlin. Opt. Phys. Mat.*, 5, 89–98 (1996).
16. E. Ginter, E. Lueder, T. Kallfass, S. Huttelmaier, M. Dobler, V. Hochholzer, D. Coates, M. Tillin, and P. Nolan, *Proc. of the 13th Int. Dis. Res. Conf.*, 13, 105–110 (1993).
17. S. D. Heavin and B. M. Fung, *Mol. Cryst. Liq. Cryst.*, 283, 83–90 (l994).
18. B. M. Fung, S. D Heavin, Z. Lin, X. Q. Jiang, J. J. Sluss, T. E. Batchman, *SPIE Proc.*, 1815, 92–97 (1992).
19. M. D. Schulte, S. J. Clarson, L. V. Natarajan, V. P. Tondiglia, D. Tomlin, and T. J. Bunning, *Liquid Crystals*, 27, 467–476 (2000).
20. Z. Huang, G. Chidichimo, G. De Filpo, A. Golemme, H. A. Hademi, and M. Santangelo, *Mol. Cryst. Liq. Cryst.*, 307, 135–141 (1997).
21. Z. Huang, G. Chidichimo, A. Golemme, H. A. Hakemi, M. Santangelo, and F. P. Nicoletta, *Liquid Crystals*, 23, 519–524 (1997).
22. C. V. Rajaram, S. D. Hudson, and L. C. Chien, *Polymer*, 39, 5315–5319 (1998).